BEN-GURION UNIVERSITY OF THE NEGEV
FACULTY OF ENGINEERING SCIENCES
DEPARTMENT OF MECHANICAL ENGINEERING

THE HALL INSTABILITY IN PLASMA FLOWS

Thesis Submitted in Partial Fulfillment of the Requirements for the M.Sc. Degree

BY: Zohar Kolberg

JANUARY 2004

BEN-GURION UNIVERSITY OF THE NEGEV
FACULTY OF ENGINEERING SCIENCES
DEPARTMENT OF MECHANICAL ENGINEERING

THE HALL INSTABILITY IN PLASMA FLOWS

Thesis Submitted in Partial Fulfillment of the Requirements for the M.Sc. Degree

BY: Zohar Kolberg

SUPERVISOR: Prof. Michael MOND

Author:

Supervisor:

Chairman of Graduate Studies Committee:

JANUARY 2004

Abstract

The Hall waves and Hall instability of ideal conducting plasmas are studied. The single fluid equations for systems with characteristic frequency larger than the ions gyro frequency, in which the Hall term is taken into account in Faraday's law, are employed. Three modes exist for waves propagating perpendicular to the magnetic field and density gradient. One of the modes is found to be always real while the other two may become unstable. The real mode and one of the unstable modes are obtained from the splitting of the fast magnetosonic mode due to the plasmas inhomogeneity while the third mode disappears in homogeneous plasma. The stable mode represents a modified whistler wave and its properties are studied and analyzed. The instability of the other two modes is shown to be driven by the plasmas acceleration. Expression for the instability threshold as well as the growth rate as functions of the wave number and the inhomogeneity scale are obtained. The growth rate depends linearly on the wave number and may lead to a catastrophic instability in the short wave length limit. However, it is shown that this problem may be resolved, by taking into account the electrons inertia, under which the growth rate attains a maximum value at a certain finite wavelength and is non zero only in a finite range of wave lengths.

It is further shown that perpendicular to the magnetic field is the direction of most unstable wave propagation within a small range about it. In addition, wave propagation in arbitrary direction is investigated and the homogeneous whistler wave is found to be destabilized due to the plasma inhomogeneity.

I would like to express my appreciation to Prof. Michael Mond and to Dr. Edward Liverts for their help and guidance

Content

1. **Introduction** 2

2. **Theoretical model** 5

2.1 The two-fluid model 5
2.2 Wave analysis 7
2.3 Single-fluid model 16
2.4 Frozen in magnetic field 21
2.5 Waves in hot homogeneous plasma 23

3. **HMHD Wave propagation perpendicular to magnetic field in inhomogeneous plasmas** 26

3.1 Basic model and assumptions 26
3.2 Condition for instability 30
3.3 Solution 32
3.4 Effect of electron inertia 38
3.5 Wave propagation almost perpendicular to magnetic field 41

4. **Three dimensional oblique waves** 45

4.1 Basic model and assumption 46
4.2 Solution 47

5. **Summary** 49

Reference 51

1. Introduction

Magnetized plasmas have been the focus of intensive investigation during the last few decades due to their relevance and importance to a wide range of laboratory and technological applications as well as to wide variety of astrophysical phenomena. Thus, modern laboratory and technological research includes such applications as thermonuclear fusion reactors, radiation sources and plasma etching in the microelectronic industry, while astrophysical phenomena range from low-frequency oscillations of the terrestrial magnetosphere through solar bursts to the acceleration of intergalactic energetic particles. In particular, wave propagation and instabilities play an important role in the evolution of magnetized plasmas under such as plasma heating in the laboratory and space as well as contributing to anomalous transport processes. Traditionally, waves that are characterized by wave lengths that are much bigger than the Larmor radius of both the electrons and the ions and by frequencies that are much higher than the gyro frequencies of the above two species, were investigated. The response of the plasma to such long wavelength low frequencies perturbations may be described by the magnetohydrodynamic (MHD) model. However, recently there is a growing interest in phenomena that are characterized by an intermediate range of frequencies and wave lengths, i.e, by wavelengths that are bigger than the Larmor radius of the electrons but smaller than that of the ions and frequencies that are higher than ions gyro frequency and smaller than that of the electrons. The response of the plasma to such perturbations is described by an extended theory that is called Hall MHD (HMHD) which is obtained from the MHD model by taking into account the Hall effect. Examples of laboratory situations in which such parameter regime is relevant are axial plasma implosion in Z-pinches in schemes to reach inertial confinement for thermonuclear purposes and in capillary discharges aimed at producing high intensity radiation in wave length range between UV and X rays. In such devices a high current is driven along their axis. This results in an azimuthal magnetic field that compresses the plasma (figure 1.1). The characteristic frequencies that describe some of the regions in devices as Z-pinch and capillary discharge are found to be in the range between the ion's to the electrons gyro frequencies and hence those regions should be described by the HMHD equations. Brushlinskii and Morozov [1] were the first to recognize the importance of the Hall instability. They have encountered large oscillations in their numerical simulation of plasma acceleration in channels and have shown that those oscillations result from the non evolutionarity of the HMHD equations due to the Hall instability. No detailed discussion, however, was presented by them. Later on, Huba [2], and Huba and hassam [3] have presented an analysis of the Rayleigh-Taylor as well as the drift instability in HMHD plasmas while Almaguer [4] investigated the role of resistivity in such instabilities. Recently, Zhu et al [5] have investigated the extension of the Ballooning modes in HMHD plasmas and their relevance in some space applications. Apart from the instabilities, the stable modes of wave propagation in HMHD plasmas were also extensively studied over the last two decades. Thus, one of those stable modes has been found to describe a fast non dissipative penetration of magnetic field into the plasma and provides the basis for modern concepts of plasma opening switches [6] and [7]. In the current work we present a detailed analysis of the stable as well as the unstable modes in accelerating inhomogeneous HMHD plasmas. In particular, we demonstrate the existence of an acceleration-driven instability and derive the conditions for its occurrence as well as its growth rate. In section 2 we lay the theoretical basis of the current analysis and discuss wave propagation in two-fluid homogeneous plasmas and discuss the transition to single fluid theories. A detailed analysis of the stable as well as the unstable modes, that propagate perpendicular to the magnetic field in inhomogeneous accelerating plasmas and close to perpendicular propagation is presented in section 3 while propagation with an arbitrary angle to the magnetic field is discussed in section 4.

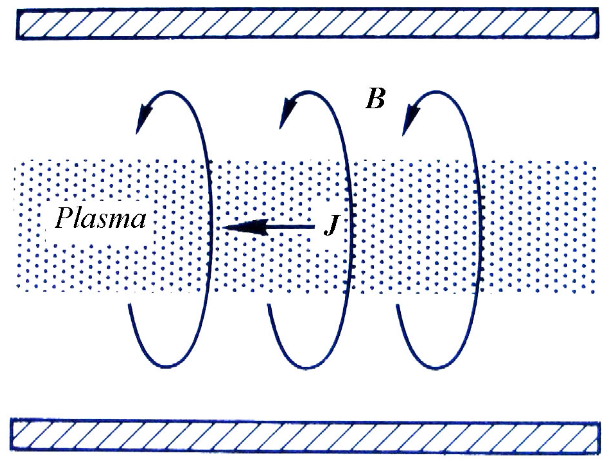

Figure 1.1 The geometry of a Z-pinch. Current is applied to the plasma in the direction shown, resulting in an azimuthal magnetic field. The consequent Lorentz force results in plasma compression.

2. Theoretical model

2.1 The two-fluid model

Consider a fully ionized plasma that is composed of singly charged ions and electrons. Each of the species is treated as a fluid that interacts with the other fluid through the self consistent electromagnetic fields. Thus, the fluid equations for the ions (properties of the ionic fluid are denoted by subscript *i*) and the electrons (properties of the electronic fluid are denoted by subscript *e*) are:

Continuity equation for ions:

$$\frac{\partial n_i}{\partial t} + \nabla(n_i \boldsymbol{U}_i) = 0 \tag{2.1}$$

Continuity equation for electrons:

$$\frac{\partial n_e}{\partial t} + \nabla(n_e \boldsymbol{U}_e) = 0 \tag{2.2}$$

Momentum equation for ions:

$$n_i m_i (\frac{\partial \boldsymbol{U}_i}{\partial t} + (\boldsymbol{U}_i \nabla)\boldsymbol{U}_i) = n_i e\left(\boldsymbol{E} + \frac{1}{c}\boldsymbol{U}_i \times \boldsymbol{B}\right) - \nabla P_i - \nabla \cdot \boldsymbol{\pi}_i + \boldsymbol{p}_{ie}$$

Momentum equation for electrons:

$$n_e m_e (\frac{\partial \boldsymbol{U}_e}{\partial t} + (\boldsymbol{U}_e \nabla)\boldsymbol{U}_e) = -n_e e\left(\boldsymbol{E} + \frac{1}{c}\boldsymbol{U}_e \times \boldsymbol{B}\right) - \nabla P_e - \nabla \cdot \boldsymbol{\pi}_e + \boldsymbol{p}_{ei}$$

The stress tensor has been split into an isotropic part P and an anisotropic part $\boldsymbol{\pi}$. The terms $\boldsymbol{p}_{ei}$ and $\boldsymbol{p}_{ie}$ represent momentum exchange between electrons and ions and according to momentum conservation these two forces must be equal and with opposite signs i,e, $\boldsymbol{p}_{ei} = -\boldsymbol{p}_{ie}$. Neglecting viscosity tensor for cold plasma (neglecting the $\boldsymbol{\pi}$ term), the equations of motion are:

for electrons:

$$n_e m_e (\frac{\partial}{\partial t}\boldsymbol{U}_e + (\boldsymbol{U}_e \nabla)\boldsymbol{U}_e) = -n_e e\left(\boldsymbol{E} + \frac{1}{c}\boldsymbol{U}_e \times \boldsymbol{B}\right) - \nabla P_e , \tag{2.3}$$

for ions:

$$n_i m_i (\frac{\partial}{\partial t}\boldsymbol{U}_i + (\boldsymbol{U}_i \nabla)\boldsymbol{U}_i) = n_i e\left(\boldsymbol{E} + \frac{1}{c}\boldsymbol{U}_i \times \boldsymbol{B}\right) - \nabla P_i \ . \tag{2.4}$$

The continuity and momentum equations are supplemented by Maxwell's equations that are given by:

Faraday's law: $$\nabla \times \boldsymbol{E} = -\frac{1}{c}\frac{\partial \boldsymbol{B}}{\partial t} \ , \tag{2.5}$$

Ampere's law: $$c\nabla \times \boldsymbol{B} - \frac{\partial E}{\partial t} = 4\pi \boldsymbol{J} \ . \tag{2.6}$$

Where the electric current density $\boldsymbol{J}$ is given by:

$$\boldsymbol{J} \ = \ e(n_i \boldsymbol{U}_i - n_e \boldsymbol{U}_e) \ . \tag{2.7}$$

In addition, equations of state are needed in order to provide relationship between the thermodynamic properties of the plasma such as the pressure, temperature and density. This will be discussed in section 2.3.

Thus, equations (2.1) – (2.7) constitute a set of partial differential equations that describe the self consistent evolution of the hydrodynamical properties of the plasma and the electromagnetic fields.

2.2 Wave analysis

The first step in wave analysis is to separate any variable in the equation into two parts: an equilibrium part and a perturbation. Assuming that the perturbations are very small in comparison to the equilibrium quantities allows linearizing the equations by neglecting powers (higher than the first) of the perturbation, leaving only terms that are of first order in the perturbations. Thus, the evolution of the perturbations is described by a set of linear partial differential equations.

All the perturbed quantities are expressed as superposition of planar waves with frequencies ω and a wave vector $\boldsymbol{k}$. Due to the linearity of the equations only a single component of the fourier decomposition need to be examined for each variable *f*.

Thus,

$$f = f^0 + f^1 e^{i(\boldsymbol{K}\cdot\boldsymbol{r}-\omega t)} \ , \tag{2.8}$$

$$\boldsymbol{k} \ = \ k_x\hat{x}+k_y\hat{y}+k_z\hat{z} \ = \ k(l_x\hat{x}+l_y\hat{y}+l_z\hat{z}) \qquad \boldsymbol{r} = x\hat{x}+y\hat{y}+z\hat{z} \ ,$$

where f^0 is the equilibrium part and f^1 is the perturbation amplitude.

Substituting expression (2.8) into equations (2.1) – (2.6) results in a linear and homogeneous set of algebraic equations for the amplitudes of the perturbed physical quantities. The condition for existence of nontrivial solution is that the determinant of the matrix of the coefficients of the above linear system is zero. This condition results in a polynomial equation for ω as a function of $\boldsymbol{k}$ and is called dispersion equation. Since there are no source terms, the solutions of the dispersion relation for ω describe all the natural modes of the waves. If some of the roots of the dispersion relation are complex there is an exponential growth of the perturbations. This exponential growth represents an instability.

It is assumed now that the plasma is cold, homogeneous and stationary. The direction of the magnetic field is chosen to be along the z axis and the x direction is chosen (without loss of generality) to be the direction of propagation of the wave perpendicular to the magnetic field, such that

$$\boldsymbol{k} = k\sin\theta\,\hat{x} + k\cos\theta\,\hat{z}\,,$$

Where θ is the angle between the magnetic field and the wave vector. Assuming that the plasma is cold means that we neglect the pressure terms in equations (2.2) – (2.3). By solving equations (2.2) and (2.3) the velocity component of electrons and ions can be found:

$$u_{\alpha x} = \frac{e_\alpha (i\omega E_x - \Omega_\alpha E_y)}{m_\alpha (\omega^2 - \Omega_\alpha^2)}\,, \tag{2.9}$$

$$u_{\alpha y} = \frac{e_\alpha (i\omega E_y + \Omega_\alpha E_x)}{m_\alpha (\omega^2 - \Omega_\alpha^2)}\,,$$

$$u_{\alpha z} = \frac{ie_\alpha E_z}{m_\alpha \omega}\,,$$

where $\alpha = i, e$ for ions and electrons respectively, and:

$$\Omega_\alpha = \frac{eB}{m_\alpha c}$$

is the gyro frequency for ions or electrons respectively.

Inserting (2.9) into (2.7) we find the current density vector, which is related to the electric field by the conductivity tensor $[\sigma]$ in the following way:

$$J_i = \sum_j \sigma_{ij} E_j\ .$$

The dielectric permittivity tensor $[\varepsilon]$ can now be found according to the following definition

$$\boldsymbol{D} = \boldsymbol{E} + \frac{4\pi i}{\omega}\boldsymbol{J} = \sum_j \varepsilon_{ij} E_j \ .$$

And is given by

$$[\varepsilon] = \begin{bmatrix} \varepsilon_1 & i\varepsilon_2 & 0 \\ -i\varepsilon_2 & \varepsilon_1 & 0 \\ 0 & 0 & \varepsilon_3 \end{bmatrix} , \tag{2.10}$$

where

$$\varepsilon_1 = 1 - \sum_\alpha \frac{\omega_{p\alpha}^2}{\omega^2 - \Omega_\alpha^2} , \qquad \varepsilon_2 = -\sum_\alpha \frac{\omega_{p\alpha}^2 \Omega_\alpha}{\omega(\omega^2 - \Omega_\alpha^2)} , \qquad \varepsilon_3 = 1 - \sum_\alpha \frac{\omega_{p\alpha}^2}{\omega^2} , \tag{2.11}$$

and

$$\omega_{p\alpha} = \sqrt{\frac{4\pi n e^2}{m_\alpha}}$$

is respectively the ions and electrons plasma frequency.

Finally, the dispersion equation can be expressed in terms of the component of the permittivity tensor (Ref. [6] and [7]):

$$An^4 + Bn^2 + C = 0 , \tag{2.12}$$

where the unknown is the refractive index defined by $n = kc/\omega$ and

$$A = \varepsilon_1 \sin^2\theta + \varepsilon_3 \cos^2\theta,$$

$$B = -\varepsilon_1\varepsilon_3(1 + \cos^2\theta) - (\varepsilon_1^2 - \varepsilon_2^2)\sin^2\theta,$$

$$C = \varepsilon_3(\varepsilon_1^2 - \varepsilon_2^2).$$

The solution of equation (2.12) is given by:

$$n^2 = \frac{-B \pm \sqrt{B^2 - 4AC}}{2A} \quad . \tag{2.13}$$

It can be shown that $B^2 - 4AC > 0$. Hence, *n*, as given by equation (2.13), may be either pure real or pure imaginary. This means that for a given real ω, *k* may be either pure real or pure imaginary. Waves cannot propagate in regions that are characterized by pure imaginary values of *k* and hence going through $n^2 = 0$, a transition is made from a region of transparency to the wave to region of evanescence. Thus, the case $n^2 = 0$ is called *cutoff* and a wave is reflected from a *cutoff* surface.

The limit of $n^2 \to \infty$ is called *resonance* frequency. Waves propagating in this frequency will be absorbed. These two conditions on n^2 establish the range of ω at which waves can propagate.

Equation (2.12) is a fifth order polynomial equation for ω and hence defines five branches of wave propagation. There are three resonances that are defined by the condition *A* = 0. For low density plasma ($\omega_{p\alpha} << \Omega_\alpha$):

$$\omega_\infty^1 = \Omega_e (1 + \frac{1}{2}\frac{\omega_{pe}^2}{\Omega_e^2}\sin^2\theta),$$

$$\omega_\infty^2 = \omega_{pe}\cos\theta,$$

$$\omega_\infty^3 = \Omega_i (1 - \frac{1}{2}\frac{m_e}{m_i}\tan^2\theta).$$

The expression for the first resonant frequency is valid for all angles. In particular, for $\theta = \pi/2$ it is called the upper hybrid frequency and given by (This expression holds for both low as well as high density plasmas):

$$\omega_\infty^1 = \sqrt{\Omega_e^2 + \omega_{pe}^2} \; .$$

The expressions for the other two resonant frequencies are valid only under the condition:

$$\cos^2\theta >> \frac{m_e}{m_i}.$$

In the case that the last inequality is not satisfied, the last two resonant frequencies for $\theta \to \pi/2$ are given by:

$$\omega_\infty^2 = \Omega_i ,$$

$$\omega_\infty^3 = \Omega_i \frac{m_i}{m_e}\cos\theta .$$

For dense plasmas the second resonant is called the lower hybrid frequency and is given by:

$$\omega_\infty^2 = \sqrt{\Omega_i\Omega_e} .$$

There are three cutoff frequencies that are determined from the condition $n^2 = 0$ and are given by:

$$\omega_0^{1,2} = \frac{1}{2}\Omega_e\left[1 \pm \sqrt{4\frac{\omega_{pe}^2}{\Omega_e^2}+1}\right],$$

$$\omega_0^3 = \omega_{pe} .$$

Propagation parallel to magnetic field

Solving for $\theta = 0$ yields:

$$n^2 = \varepsilon_1 \pm \varepsilon_2 = \begin{cases} 1 - \dfrac{\omega_{pe}^2}{\omega(\omega - \Omega_e)} - \dfrac{\omega_{pi}^2}{\omega(\omega + \Omega_i)} \\ 1 - \dfrac{\omega_{pe}^2}{\omega(\omega + \Omega_e)} - \dfrac{\omega_{pi}^2}{\omega(\omega - \Omega_i)} \end{cases} . \qquad (2.14)$$

One of the modes is given by:

$$\omega = \sqrt{\omega_{pe}^2 + \omega_{pi}^2}$$

which represents langmuir oscillations. Solution (2.14) for the rest four modes is shown in figure 2.1 while the four roots of (2.12) as a function of k are shown in figure 2.2, the latter are also called branches of wave propagation.

In the high frequency range, there are two modes that can be determined by neglecting the ionic contribution to the dielectric permittivity tensor. Both modes are circularly polarized in the plane perpendicular to the magnetic field, one of which is right hand polarized and has a resonant frequency that is the electron gyro frequency and the other is left hand polarized and has a resonant frequency that is the ions gyro frequency. The first is called extraordinary wave and it rotates in the same sense as the electrons and hence, for frequencies near the electron gyro frequencies the electrons can absorb energy from the wave. The second mode is called ordinary wave and regarding the electrons, this mode does not have a resonant since the electric field rotates in opposite sense to the electrons. It can be seen in figure (2.1) that for very high frequencies both waves behave like electromagnetic waves in vacuum i,e, $n^2 = 1$ or $\omega = kc$.

For frequencies below the electrons gyro frequencies the ionic contribution should be retain. There are two branches of electromagnetic waves in that limit ($\omega << \Omega_i$):

the Alfven wave:

$$\omega = kV_A \cos\theta ,$$

and the fast magnetosonic wave:

$$\omega = kV_A ,$$

where

$$V_A = \frac{B}{4\pi nm_i} .$$

is the Alfven velocity. Both expressions are valid for any angle of propagation.

For intermediate frequency range such that the frequencies approach the ions gyro frequency, the refractive index of the Alfven wave tends to infinity, which means that it has a resonant for that frequency. In that intermediate range the Alfven branch is often called the ion cyclotron wave. For the fast magnetosonic wave in the range ($\Omega_i << \omega << \Omega_e$) the dispersion relation is called the Whistler wave and is given by:

$$\omega = \frac{k^2 V_A^2}{\Omega_i} \cos\theta .$$

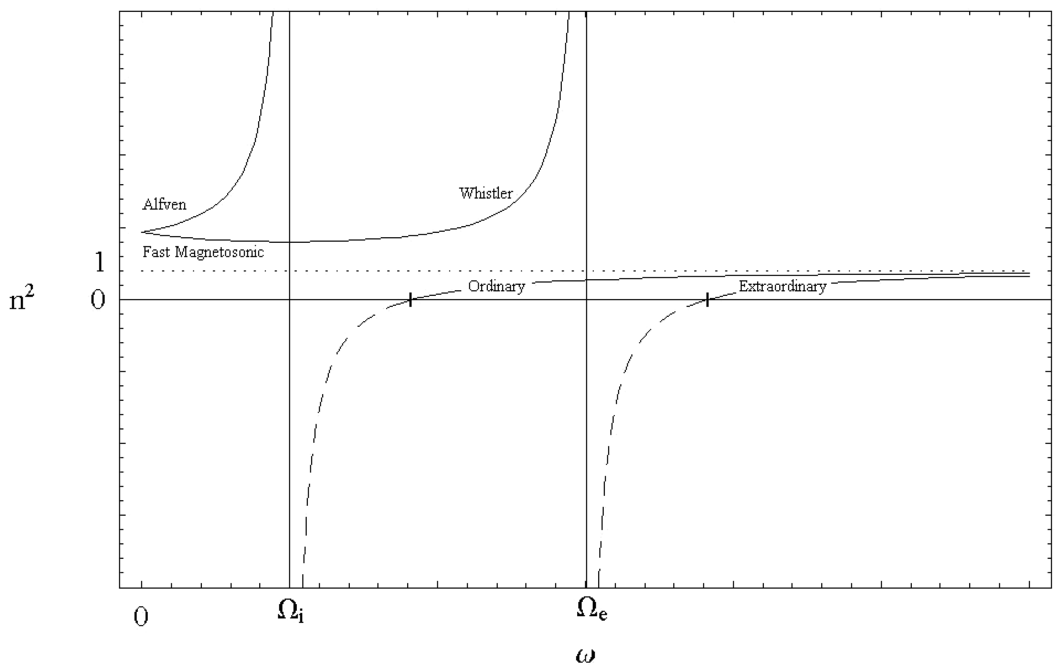

Figure 2.1: The refractive index as a function of the frequency ω for propagation parallel to the magnetic field.

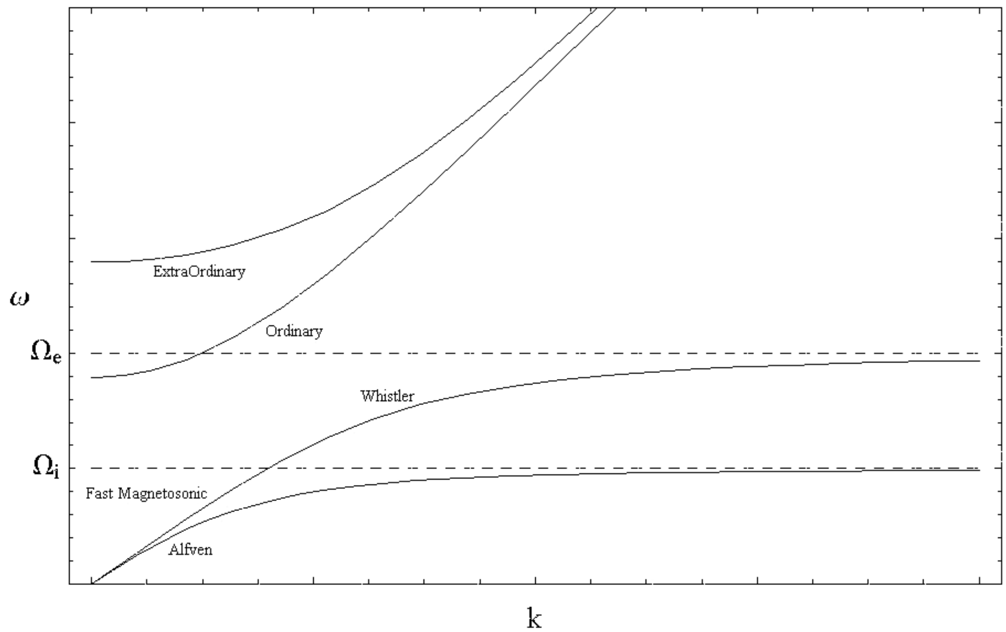

Figure 2.2: The frequency ω as a function of k for propagation parallel to the magnetic field.

Propagation perpendicular to magnetic field

Solving for $\theta = \pi/2$ yields:

$$n^2 = \begin{cases} \varepsilon_3 \\ \dfrac{\varepsilon_1^2 - \varepsilon_2^2}{\varepsilon_1} \end{cases} . \tag{2.15}$$

In the high frequency limit, the perturbed electric field of the ordinary mode is along the magnetic field and hence, the later does not influence the propagation of that mode. This is the reason it is called ordinary mode. The extraordinary mode has a resonant frequency which is the upper hybrid frequency and it exists on both its sides with two cutoffs. The extraordinary mode has components of the perturbed electric field both parallel as well perpendicular to $\boldsymbol{k}$. For very high frequencies though, it becomes transverse electromagnetic wave in vacuum ($\omega = kc$). In the low and intermediate limits, the Alfven wave disappears and the fast magneto-sonic branch has a resonance at the lower hybrid frequency.

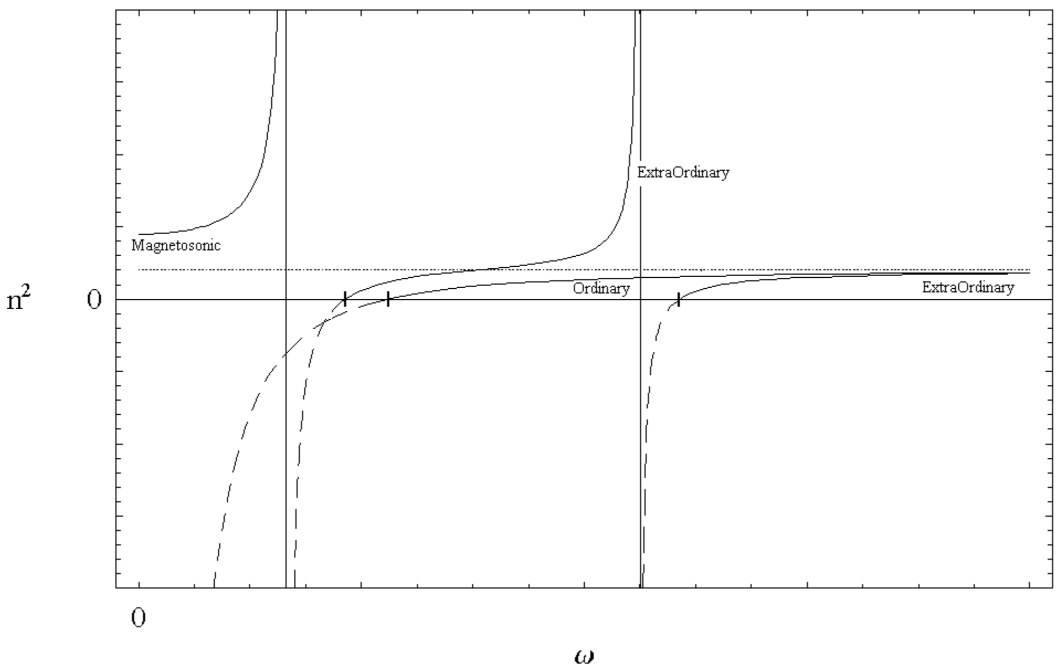

Figure 2.3: The refractive index as a function of the frequency ω for propagation perpendicular to the magnetic field.

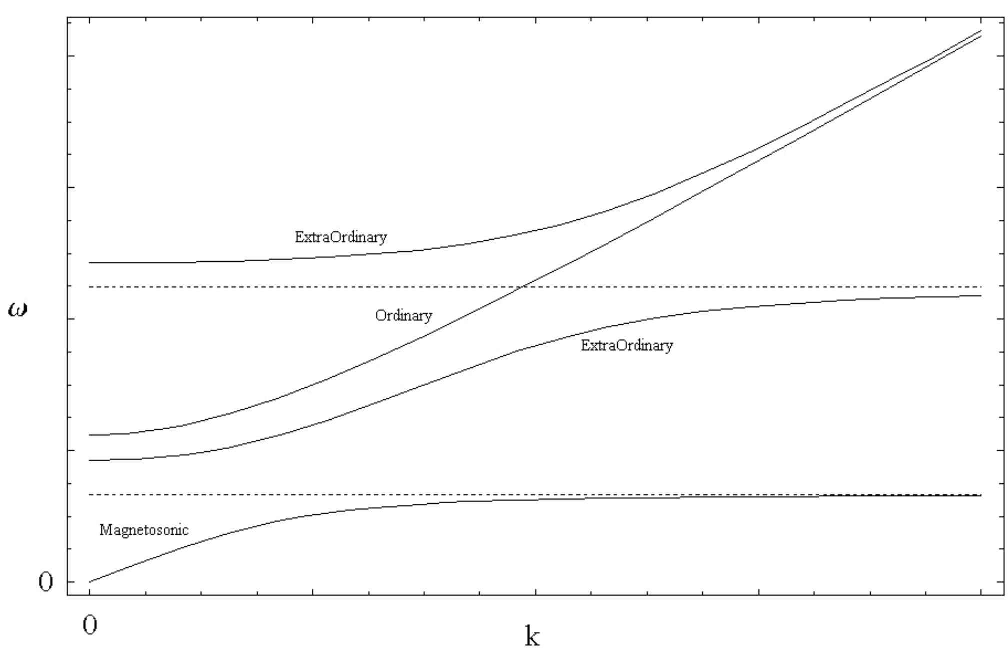

Figure 2.4: The frequency ω as a function of *k* for propagation perpendicular to the magnetic field.

2.3 Single-fluid model

So far the electrons and the ions have been considered as two separate fluids that interact with each other through the electromagnetic waves. However, for some purposes both ions and electrons may be viewed as a single effective fluid. The single fluid is characterized by an average mass density and average fluid velocity that are defined in the following way:

$$\rho \equiv n_i m_i + n_e m_e ,$$

$$\boldsymbol{U} \equiv \frac{n_i m_i \boldsymbol{U}_i + n_e m_e \boldsymbol{U}_e}{n_i m_i + n_e m_e} .$$

And a pressure that is the sum of the partial pressures of the ions and the electrons:

$$P = P_i + P_e .$$

Due to the large ratio of the ion mass to electron mass the fluid properties are approximately given by those of the ion fluid, taking into account quasineutrality, i,e, $n_i = n_e = n$:

$$\rho \approx n m_i ,$$

$$\boldsymbol{U} \approx \boldsymbol{U}_i .$$

The equations that govern the motion of the single fluid may be obtained in the following way: the mass conservation equation for the fluid is derived by multiplying the continuity equations (2.1) and (2.2) for ions and electrons by the electrons and ions mass respectively, and adding the two equations. The result is:

$$\frac{\partial \rho}{\partial t} + \nabla \cdot (\rho \boldsymbol{U}) = 0 . \qquad (2.16)$$

The momentum equation for the single fluid is obtained by adding (2.3) and (2.4):

$$\rho\frac{\partial \boldsymbol{U}}{\partial t}+\rho(\boldsymbol{U}\nabla)\boldsymbol{U}=\frac{\boldsymbol{J}\times\boldsymbol{B}}{c}-\nabla P\,. \tag{2.17}$$

An additional equation is obtained by replacing $\boldsymbol{U}_e$ in the momentum equation for the electrons (2.3) by expression derived from equation (2.7):

$$\boldsymbol{U}_e=\boldsymbol{U}-\frac{\boldsymbol{J}}{ne}\,,$$

results in:

$$\boldsymbol{E}=-\frac{1}{c}\boldsymbol{U}\times\boldsymbol{B}+\frac{\boldsymbol{J}\times\boldsymbol{B}}{nec}-\frac{\nabla P_e}{ne}-m_e\left\{\frac{\partial}{\partial t}\left(\boldsymbol{U}-\frac{\boldsymbol{J}}{ne}\right)\right\}. \tag{2.18}$$

Neglecting electron inertia results the following equation:

$$\boldsymbol{E}=-\frac{1}{c}\boldsymbol{U}\times\boldsymbol{B}+\frac{\boldsymbol{J}\times\boldsymbol{B}}{nec}-\frac{\nabla P_e}{ne}\,,$$

which is also known as the generalized ohms law.

In order to determined under what circumstances the term that represents the electron inertia may be neglected we examine the ratio of inertia term to the Lorentz force term in the electron momentum equation. This ratio is given by:

$$\frac{\omega m_e c}{Be}=\frac{\omega}{\Omega_e}\,.$$

Thus in the limit of $\Omega_e \gg \omega$ electron inertia can be neglected.

Applying the curl operator to both sides of equation (2.18) and inserting Faraday's law results in:

$$\frac{\partial \boldsymbol{B}}{\partial t} - \nabla \times (\boldsymbol{U} \times \boldsymbol{B}) + m\nabla \times (\frac{\boldsymbol{J} \times \boldsymbol{B}}{\rho e}) + \frac{c}{n^2 e}\nabla n \times \nabla P_e = 0. \qquad (2.19)$$

The set of hydrodynamic and Maxwell's equations are supplemented by equations of state. Thus, assuming that the plasma is an ideal gas that is characterized by a specific heat ratio γ, the following thermodynamic relations are employed:

$$P = \rho RT \ ,$$

and

$$P = C(s) \cdot \rho^{\gamma} .$$

Under either isothermal or isentropic flow, the above two relations result in:

$$\nabla P = a^2 \nabla \rho , \qquad (2.20)$$

where a is either the isothermal or isentropic sound velocity and C is a function of the entropy s.

With the definition of (2.20) the last term in equation (2.19) is equal zero
To summarize, the partial differential equations that govern the evolution of the plasma within the single fluid approach are:

$$\frac{\partial \rho}{\partial t} + \nabla(\rho \boldsymbol{U}) = 0 , \qquad (2.21a)$$

$$\frac{\partial \boldsymbol{B}}{\partial t} - \nabla \times (\boldsymbol{U} \times \boldsymbol{B}) + m\nabla \times (\frac{\boldsymbol{J} \times \boldsymbol{B}}{\rho e}) = 0 , \qquad (2.21b)$$

$$\frac{\partial}{\partial t}\boldsymbol{U} + (\boldsymbol{U}\nabla)\boldsymbol{U} - \frac{\boldsymbol{J} \times \boldsymbol{B}}{\rho c} + a^2 \frac{\nabla \rho}{\rho} = 0 . \qquad (2.21c)$$

MHD and HMHD

The third term on the left hand side of equation (2.21b) is known in the literature as the Hall term. In order to examine its magnitude relative to the other terms in the equation, the following estimate is carried out:

$$\frac{m\nabla\times(\dfrac{\boldsymbol{J}\times\boldsymbol{B}}{\rho e})}{\dfrac{\partial\boldsymbol{B}}{\partial t}} \sim \frac{mck^2B^2}{-i\omega B4\pi\rho e} \approx \frac{k^2V_A^2}{\Omega_i^2}\frac{\Omega_i}{\omega}. \tag{2.22}$$

As may be realized from the previous section, in the low frequency limit, i,e, $\omega << \Omega_i$, ω is of the order of kV_A. Hence, the ratio in (2.22) is of the order of ω/Ω_i, which is much smaller than unity. This means that the Hall term may be neglected in equation (2.21b). The model that result from omitting the Hall term from equation (2.21b) is called Magnetohydrodynamic (MHD) and is characterized by $\omega << \Omega_i << \Omega_e$ which means that both ions and electrons are magnetized.

The term $k^2{V_A}^2/\Omega_i^2$ is sometimes called the Hall parameter and it can also be written in terms of the plasma ion frequency:

$$\frac{k^2{V_A}^2}{{\Omega_i}^2} = \frac{k^2c^2}{{\omega_{pi}}^2} \ .$$

Turning now to the higher frequency range, i,e, $\omega >> \Omega_i$ (but still neglecting electron inertia so that $\omega << \Omega_e$) it is seen in (2.22) that $k^2V_A^2/\Omega_i >> 1$ in such a way that the ratio in (2.22) is of the order of unity or higher. Hence, the Hall term has to be retained in equation (2.21b). The resulting model is called Hall Magnetohydrodynamic (HMHD) and describes magnetized electrons ($\omega << \Omega_e$) and unmagnetized ions ($\omega >> \Omega_i$).

Knowing that $V_A = k\omega$ for Alfven waves phase velocity it follows that for the MHD approximation k must be small in order to keep these terms small. That corresponds to long waves in the MHD limit.

In the MHD limit we are left with the single fluid system of equations which contain the single fluid momentum equation, Ohms law and continuity equation.

Finally, we would like to express the current density $\boldsymbol{J}$ in terms of the magnetic field $\boldsymbol{B}$. In order to do that we examine the ratio of the two terms on the left hand side of Ampere's law (2.6):

$$\frac{\frac{\partial E}{\partial t}}{c\nabla\times\boldsymbol{B}} \propto \frac{E\omega}{cBk} .$$

From Faraday's law it follows:

$$Ek \propto \frac{B\omega}{c} \rightarrow \frac{E}{B} \propto \frac{\omega}{kc}$$

$$\rightarrow \quad \frac{\frac{\partial E}{\partial t}}{c\nabla\times\boldsymbol{B}} \propto \left(\frac{\omega}{kc}\right)^2 \propto \frac{1}{n^2} .$$

It follows that for $n^2 >> 1$, the displacement current may be neglected. Thus, the resulting HMHD equations are:

$$\frac{\partial}{\partial t}\boldsymbol{U} + (\boldsymbol{U}\nabla)\boldsymbol{U} + a^2\frac{\nabla\rho}{\rho} - \frac{1}{4\pi\rho}(\nabla\times\boldsymbol{B})\times\boldsymbol{B} = 0 , \tag{2.23a}$$

$$\frac{\partial\boldsymbol{B}}{\partial t} - \nabla\times(\boldsymbol{U}\times\boldsymbol{B}) + \underbrace{cm\nabla\times\left[\frac{(\nabla\times\boldsymbol{B})\times\boldsymbol{B}}{4\pi\rho e}\right]}_{HMHD\ Term} = 0 , \tag{2.23b}$$

$$\frac{\partial\rho}{\partial t} + \nabla(\rho\boldsymbol{U}) = 0 . \tag{2.23c}$$

2.4 Frozen in magnetic field

In order to investigate the relative motion of the magnetic field lines and the plasma we examine the time variation of the magnetic field flux. The latter is defined for an arbitrary surface in the following way:

$$\phi = \int_S \boldsymbol{B} \cdot d\boldsymbol{S} \, .$$

Assuming that the surface is moving with a velocity $\boldsymbol{V}$, ϕ changes due to time variation in $\boldsymbol{B}$ as well as due to the change of the surface itself, as a result of its motion effect of convection. Thus, the total rate of change of ϕ is given by:

$$\frac{d\phi}{dt} = \int_S \frac{\partial \boldsymbol{B}}{\partial t} \cdot d\boldsymbol{S} + \int_S \boldsymbol{B} \cdot \frac{\partial \boldsymbol{S}}{\partial t} \, .$$

Letting $\boldsymbol{dl}$ be a unit vector lying on the circumference of S. Due to the velocity $\boldsymbol{V}$ the surface sweeps out an area $\boldsymbol{V}dt \times \boldsymbol{dl}$ in time dt (figure 2.5). Applying Gauss theorem to the volume created by the motion of the surface yields:

$$\int_S \boldsymbol{B} \cdot \frac{\partial \boldsymbol{S}}{\partial t} = \oint \boldsymbol{B} \cdot (\boldsymbol{V} \times d\boldsymbol{l})$$

Substituting for the change in the surface S and summing along the circumference of S:

$$\frac{d\phi}{dt} = \int_S \frac{d\boldsymbol{B}}{dt} \cdot d\boldsymbol{S} + \oint \boldsymbol{B} \cdot (\boldsymbol{V} \times d\boldsymbol{l}) \, .$$

Finally, using stokes theorem for the second term on the left hand side results in:

$$\frac{d\phi}{dt} = \int_S \left[\frac{\partial \boldsymbol{B}}{\partial t} - \nabla \times (\boldsymbol{V} \times \boldsymbol{B}) \right] \cdot d\boldsymbol{S} \, . \qquad (2.24)$$

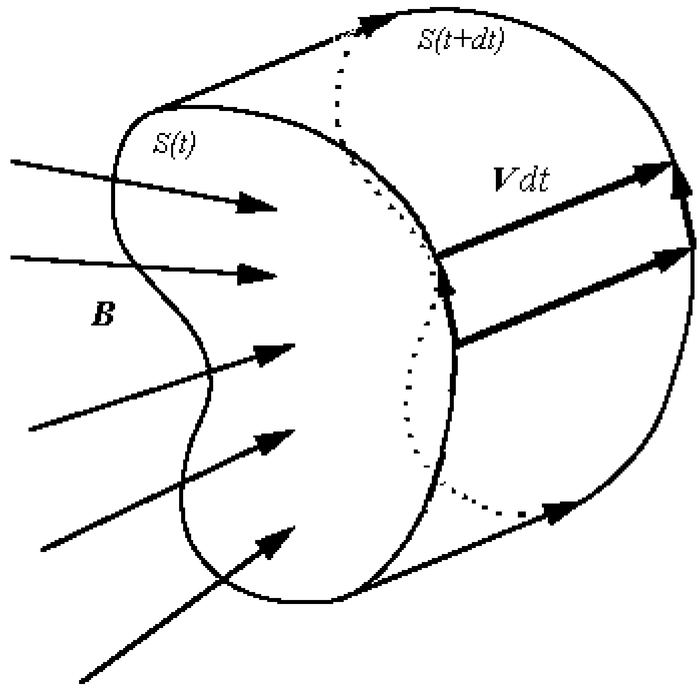

Figure 2.5: Due to the velocity ***V*** the surface *S* sweeps out an area $\boldsymbol{V}dt \times \boldsymbol{dl}$ in time *dt*.

Consider now the MHD model and assume that ***V*** is the fluid average velocity ***U***. In this case, using equation (2.21b) it is readily seen that $d\phi/dt = 0$. This means that the magnetic field lines are convected along with the fluid mass elements and are thus said to be frozen into the fluid.

Turning now to the HMHD model, we assume that the velocity ***V*** is the electrons velocity $\boldsymbol{U}_e$. Expressing $\boldsymbol{U}_e$ in terms of ***U*** and ***J*** and inserting the result into equation (2.24) yields:

$$\frac{d\phi}{dt} = \int_S \left[\frac{\partial \boldsymbol{B}}{\partial t} - \nabla \times (\boldsymbol{U} \times \boldsymbol{B}) + \nabla \times (\frac{\boldsymbol{J} \times \boldsymbol{B}}{ne}) \right] \cdot d\boldsymbol{S} \;= 0\,. \qquad (2.25)$$

Equation (2.25) means that the magnetic field is now frozen into the electronic fluid. In this sense, HMHD, in contrast to MHD, is not a truly single fluid model and as will be seen later this gives rise to phenomena such as non diffusive magnetic field penetration that are unique to the parameter range that defines the HMHD model.

2.5 Waves in hot homogeneous plasmas

MHD Waves in homogeneous plasmas

Considering equations (2.23a) – (2.23c) in the MHD limit and taking into account the pressure term in (2.23a) we obtain the following dispersion equation:

$$\omega^6 - \omega^4 k^2 (a^2 + {V_A}^2 (1+\cos^2\theta)) + \omega^2 k^4 {V_A}^2 \cos^2\theta ({V_A}^2 + 2a^2) - k^6 {V_A}^4 a^2 \cos^4\theta \ , \qquad (2.26)$$

where θ is the angle between the wave and the magnetic field. $\boldsymbol{V_A}$ is the Alfven velocity that was defined in the section 2.2. Thus, we obtain three possible modes:

Alfven waves

$$\omega = kV_A \cos\theta \,,$$

and fast magnetosonic and slow magnetosonic waves (correspond to the $\pm$ signs respectively):

$$\omega^2 = k^2 \frac{1}{2}\left[(a^2 + {V_A}^2) \pm \sqrt{(a^2 + {V_A}^2)^2 - 4a^2 {V_A}^2 \cos^2\theta} \right]. \qquad (2.27)$$

Two limits of equation (2.27) are of interest, namely, parallel and perpendicular to the magnetic field propagation.

Parallel propagation to magnetic field; i,e, $\theta = 0$:

The Alfven wave turns into $\omega = kV_A$.

Fast Magnetosonic and Slow Magnetosonic modes turns into the Alfven Waves and sound waves.

The perturbations that characterize the Alfven wave are the velocity component perpendicular to the magnetic field and a magnetic field perturbation which is also perpendicular to the unperturbed magnetic field. The relation between those perturbations is given by:

$$\frac{u_x^1}{V_A} = \frac{b_x^1}{B},$$

where the subscript x denotes the direction perpendicular to the unperturbed magnetic field. This result emphasizes the fact that the magnetic field is frozen into the ions fluid in the MHD model.

Perpendicular propagation to magnetic field; i,e, $\theta = \pi/2$:

The Alfven and the Slow Magnetosonic waves disappear and only the Fast Magnetosonic mode exists and is given by:

$$\omega = k\sqrt{a^2 + V_A{}^2}$$

For this magnetosonic wave we can write: $V_{ph}^2 = \frac{1}{\rho}(a^2\rho + \frac{B^2}{4\pi})$. This phase velocity is exactly like sound waves velocity but instead of thermal pressure we have the total pressure which is the sum of the thermal and magnetic pressures.

The perturbations that characterize the fast magnetosonic wave are of the velocity component perpendicular to the magnetic field, a magnetic field perturbation which is parallel to the unperturbed magnetic field and a perturbation in the density. The perturbations as functions of the magnetic field perturbation are given by:

$$\frac{u_x^1}{\sqrt{V_A^2 + a^2}} = \frac{b_z^1}{B},$$

and

$$\frac{\rho^1}{\rho} = \frac{b_z^1}{B},$$

where the subscript z denotes the direction parallel to the unperturbed magnetic field.

These waves are longitudinal waves, with a pressure wave that moves in the wave direction like sound waves.

HMHD Waves in homogeneous plasmas

The HMHD model differs from the two fluid one by neglecting in the HMHD the electrons inertia, hence, the high frequency modes that were discussed in section 2.2 do not exist within the framework of the HMHD model. Thus, in HMHD the parallel propagation modes are the fast magnetosonic waves that are turns into whistler modes for high k's with resonance at Ω_e and Alfven waves with resonance at Ω_i (see figure 2.2). The only non evanescent perpendicular mode is the fast magnetosonic wave with a resonance at the lower hybrid frequency (see figure 2.4).

3. HMHD Wave propagation perpendicular to magnetic field in inhomogeneous plasma.

Until now, the wave analysis that was carried out in the previous sections for homogeneous plasma is well known and can be found in papers and text books (references [6] and [7]). In this chapter a detailed analysis of waves in the HMHD limit for inhomogeneous plasma is presented. This constitutes the main contribution of this work.

3.1 Basic model and assumptions.

In this section, wave propagation in inhomogeneous plasmas is considered such that the wave vector is perpendicular to the magnetic field as well to the density gradient (Figure 3.1). The motivation for investigating such geometry is drawn from such devices as Z - pinch and capillary discharge, in which both the plasma flow as well as the density gradient are aligned along the radial direction, the magnetic field is azimuthal, while short scale perturbations along the z - axis are experimentally observed.

Thus, the unperturbed state is characterized by a magnetic field that is aligned along the z axis and a density gradient (which is in the direction of the flow) along the x axis. Another simplification is made by taking the magnetic field gradient to be aligned with density gradient:

$$\boldsymbol{B} = B(x)\hat{z}, \qquad \rho = \rho(x), \qquad \boldsymbol{k} = k\hat{y}.$$

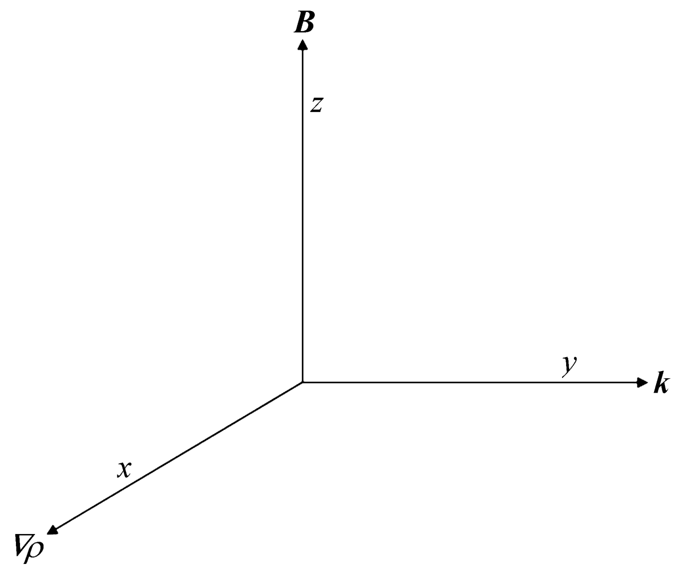

Figure 3.1: The wave vector is perpendicular to the magnetic field as well to the density gradient.

As a result, the acceleration of the plasma is in the x direction. From equation (2.21c) for steady state:

$$\frac{d\boldsymbol{U}}{dt} = (\boldsymbol{U}\cdot\nabla)\boldsymbol{U} = \frac{\boldsymbol{J}\times\boldsymbol{B}}{\rho c} - a^2\frac{\nabla\rho}{\rho} = -\frac{1}{\rho}\left[\frac{\nabla B^2}{8\pi} + a^2\nabla\rho\right]. \tag{3.1}$$

The perturbations are written in the following form:

$$\begin{aligned} \boldsymbol{B}_1 &= (b_x{}^1\hat{x} + b_y{}^1\hat{y} + b_z{}^1\hat{z})e^{i(ky-\omega t)}, \\ \boldsymbol{U}_1 &= (u_x{}^1\hat{x} + u_y{}^1\hat{y} + u_z{}^1\hat{z})e^{i(ky-\omega t)}, \\ \rho_1 &= \rho^1 e^{i(ky-\omega t)}. \end{aligned} \tag{3.2}$$

It is further assumed that the perturbations wave length $2\pi/k$, is much smaller than the characteristic scale of the inhomogeneity of the unperturbed state, such that:

$$kL_n >> 1 \ , \tag{3.3}$$

where

$$1/L_n \sim \nabla\rho/\rho \sim \nabla B/B\,.$$

Assumption (3.3) is also known as the method of frozen coefficient and means that the coefficients of the perturbations are almost constant in compare with the perturbation. Inserting (3.2) into equations (2.23a) - (2.23c), transforming to a local frame of reference that moves with the plasma and linearizing around the unperturbed state yields the following set of 7 equations:

$$b_x^1(4e\pi\rho\omega + ckmB') = 0\,, \tag{3.4a}$$

$$b_y^1 = \frac{imc(B'\rho' - \rho B'')}{4e\pi\rho^2\omega} b_x^1\,, \tag{3.4b}$$

$$\left(-i\omega - ik\frac{Bmc\rho'}{4\pi\rho^2 e}\right) b_z^1 + B'u_x^1 - ikBu_y^1 + ik\frac{BmcB'}{4\pi\rho^2 e}\rho^1 = 0\ , \tag{3.4c}$$

$$\frac{B'}{4\pi\rho} b_z^1 - i\omega u_x^1 = 0\,, \tag{3.4d}$$

$$\frac{kB}{4\pi\rho} b_z^1 + \omega u_y^1 + \frac{ka^2}{\rho}\rho^1 = 0\,, \tag{3.4e}$$

$$u_z^1 = \frac{iB'}{4\pi\rho\omega} b_x^1\,, \tag{3.4f}$$

$$u_x^1\rho' - ik\rho u_y^1 - i\omega\rho^1 = 0\,, \tag{3.4g}$$

where the prime denotes differentiation with respect to the argument. Equations (3.4a), (3.4b) and (3.4f) form a decoupled subsystem that gives a non zero solution for the quantities b_y^1 and u_z^1 in terms of b_x^1 along with $b_z^1 = u_x^1 = u_y^1 = 0$. This subsystem corresponds to the following relation between ω and k:

$$\omega = k\frac{V_A^2}{\Omega_i}\left(\frac{(\boldsymbol{U}\cdot\nabla)\boldsymbol{U}}{V_A{}^2} + \frac{\beta}{L_n}\right), \tag{3.5}$$

where

$$\beta = \frac{a^2}{{V_A}^2}.$$

This is a new stable mode which depends on the inhomogeneity of the plasma and disappears in homogeneous and constant flow plasmas. The rest of the eigen frequencies and eigen functions are obtained by assuming that:

$$b_x^1 = b_y^1 = u_z^1 = 0.$$

Thus, using once again the condition $k >> 1/L_n$ the solution for the second decoupled subsystem, i,e: equations (3.1d) , (3.1e) and (3.1g), may be expressed in terms of the perturbed magnetic field in the $\hat{z}$ direction.

$$\rho^1 = -\frac{Bk^2}{4\pi(a^2k^2 - \omega^2)} b_z^1, \tag{3.6a}$$

$$u_y^1 = \frac{kB\omega}{4\pi\rho(a^2k^2 - \omega^2)} b_z^1 , \tag{3.6b}$$

$$u_x^1 = -\frac{iB'}{4\pi\rho\omega} b_z^1 . \tag{3.6c}$$

Substituting (3.6a) – (3.6c) into (3.4c) results the following dispersion equation that provides a relationship between ω and *k*.

$$\omega^3 + \omega^2 \frac{k{V_A}^2}{\Omega_i L_n} - \omega k^2 {V_A}^2 (1+\beta) + \frac{k^3{V_A}^2}{\Omega_i} (\boldsymbol{U} \cdot \nabla)\boldsymbol{U} = 0 . \tag{3.7}$$

Equation (3.7) is an equation of order three with three possible roots one of which has to be real and the other two may be either real or a pair of complex -conjugate roots. In the latter case, one of the two complex roots given rise to an unbounded exponential growth of the perturbations, i.e, an instability.

3.2 Conditions for instability

Conditions for complex roots for equation (3.4) can be obtained as follows:

For any polynomial of order 3 of the form: $x^3 + a_1 x^2 + a_2 x + a_3 = 0$.

Changing variable:

$$x = -\frac{a_1}{3} + y,$$

results in:

$$y^3 + 3py + 2q = 0,$$

where

$$p = \frac{1}{3}(a_2 - \frac{a_1^{\ 2}}{3}), \qquad q = \frac{1}{3}(a_3 - \frac{a_1 a_2}{3} + \frac{2a_1^{\ 3}}{27}) .$$

If $p < 0$ the conditions for complex roots is $D > 0$, where

$$D = q^2 + p^3$$

For equation (3.7) the coefficient p and q are given by:

$$p = \frac{1}{3}\left[-k^2 V_A^{\ 2}(1+\beta) - \frac{k^2 V_A^{\ 4}}{3L_n^{\ 2}\Omega_i^{\ 2}} \right] \approx -\frac{k^2 V_A^{\ 4}}{9L_n^{\ 2}\Omega_i^{\ 2}} < 0$$

$$q = \frac{k^3 V_A^{\ 3}}{2}\left[\frac{\boldsymbol{U}\cdot\nabla\boldsymbol{U}}{\Omega_i V_A} + \frac{V_A(1+\beta)}{3L_n\Omega_i} + \frac{2V_A^{\ 3}}{27\,L_n^{\ 3}\Omega_i^{\ 3}} \right] \approx \frac{k^3 V_A^{\ 3}}{2}\left[\frac{\boldsymbol{U}\cdot\nabla\boldsymbol{U}}{\Omega_i V_A} + \frac{2V_A^{\ 3}}{27\,L_n^{\ 3}\Omega_i^{\ 3}} \right]$$

Consequently, the condition $D > 0$ yields the following condition on the acceleration for instability:

$$(\boldsymbol{U}\cdot\nabla\boldsymbol{U})^2 + b\,(\boldsymbol{U}\cdot\nabla\boldsymbol{U}) + c > 0\ , \tag{3.8}$$

where

$$b = \frac{2V_A^{\ 2}}{27L_n^{\ 3}\Omega_i^{\ 2}}\left(9L_n^{\ 2}\Omega_i^{\ 2}(1+\beta) - 2V_A^{\ 2}\right)$$

and

$$c = -\frac{V_A^{\ 2}(1+\beta)}{27L_n^{\ 2}}\left(V_A^{\ 2} + 4L_n^{\ 2}\Omega_i^{\ 2}(1+\beta)\right).$$

The solution of (3.8) is given by:

$$\boldsymbol{U}\cdot\nabla\boldsymbol{U} = \frac{1}{2}\left[-b \pm \sqrt{b^2 - 4c}\right],$$

which means that if the acceleration satisfied the following inequalities:

$$\boldsymbol{U}\cdot\nabla\boldsymbol{U} < \frac{1}{2}\left[-b - \sqrt{b^2 - 4c}\right]$$

or

$$\boldsymbol{U}\cdot\nabla\boldsymbol{U} > \frac{1}{2}\left[-b + \sqrt{b^2 - 4c}\right].$$

Equation (3.7) posses two complex conjugated roots. In the HMHD limit $V_A/\Omega_i L_n >> 1$ these conditions are:

$$\boldsymbol{U}\cdot\nabla\boldsymbol{U} > \frac{1}{4}L_n\Omega_i^{\ 2}(1+\beta)^2 \tag{3.9a}$$

or

$$\boldsymbol{U}\cdot\nabla\boldsymbol{U} < -\frac{4V_A^{\ 4}}{27L_n^3\Omega_i^{\ 2}}. \tag{3.9b}$$

It is noted that if L_n is taken to be negative, the inequality signs change.

3.3 Solution

Figure 3.2 presents a plot of the roots of equation (3.7). The roots are marked with numbers 1-3. In the MHD limit ($kV_A / \Omega_i << 1$), roots 1 and 2 converge to the fast magnetosonic wave. In the HMHD limit, it is one of these roots that becomes unstable. The imaginary part of this root is shown with the dashed line.

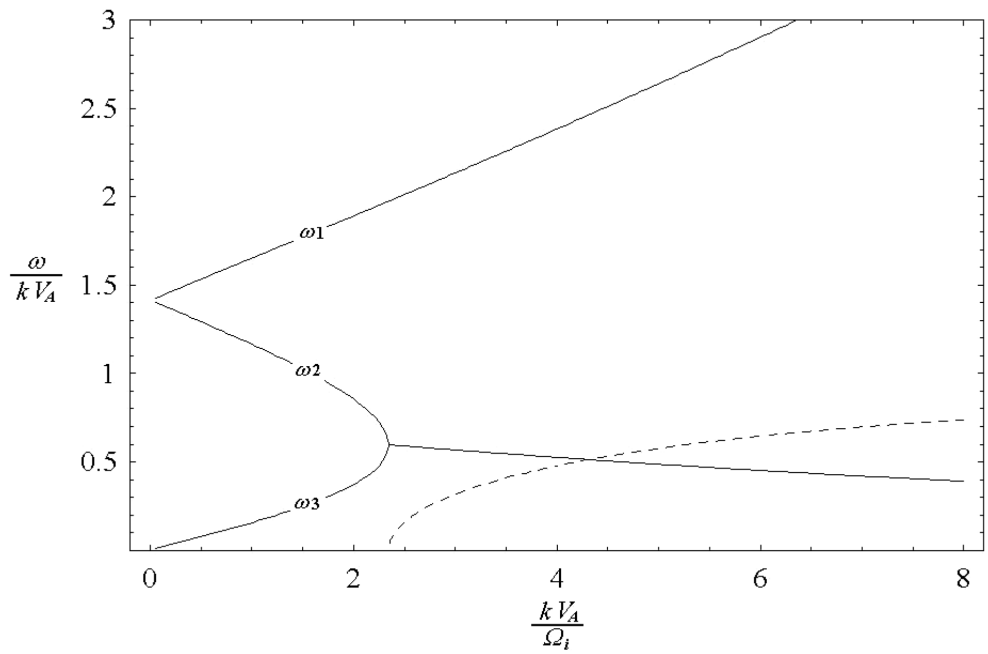

Figure 3.2: Plot of the roots of Eq. (3.7). The dashed line represents the imaginary part of the complex conjugate roots.
The parameters for this plot are: $\beta = 1$, $kL_n = 3$, $U \cdot \nabla U / L_n k^2 V_A^2 = 0.1$

Stable mode

The mode that is denoted by subscript 1 in figure 3.2 remains always stable i.e, ω_1 is always real. In the MHD limit $V_A / L_n \Omega_i << 1$, this mode may be presented as follows:

$$\omega_1 = kV_A\left\{\sqrt{1+\beta} + \frac{\boldsymbol{U}\cdot\nabla\boldsymbol{U}}{2L_n\varOmega_i^2(1+\beta)}\frac{L_n\varOmega_i}{V_A} + O[\frac{V_A}{L_n\varOmega_i}]\right\}. \tag{3.10}$$

For homogeneous plasma this root turns into the fast magnetosonic wave.

In the HMHD limit $V_A / L_n\varOmega_i >> 1$:

$$\omega_1 = kL_n\Omega_i\left\{\frac{V_A^2}{L_n^2\Omega_i^2} + \left(\frac{\boldsymbol{U}\cdot\nabla\boldsymbol{U}}{L_n\Omega_i^2} - \frac{(1+\beta)^2}{4}\right)\left(\frac{L_n\Omega_i}{V_A}\right)^2\right\}. \tag{3.11}$$

The first order term of ω_1 in (3.11) does not depend on acceleration and looks like modified whistler where k/L_n replaces k^2. As the acceleration grows the second order term will gradually become effective.

Substituting the first order term of ω_1 in (3.11) into (3.6a) - (3.6c) yields:

$$\frac{\rho^1}{\rho} \approx \left(\frac{\Omega_i L_n}{V_A}\right)^2 \frac{b_z^1}{B} \tag{3.12}$$

and

$$\frac{j_x^1}{J} \approx \left(\frac{kV_A}{\varOmega_i}\right)^2 \frac{u_x^1}{V_{ph}},$$

where

$$V_{ph} = \omega/k\,.$$

Relations (3.12) means that the relative perturbations in the ionic fluid are much smaller than those in the electronic fluid and the magnetic field. Thus, while the ions are practically immobile in this mode, the electrons are moving and carrying with them the perturbations in the magnetic field, as was shown in section 2.4. Hence, this mode is called magnetic field penetration mode. It is further noticed that its phase velocity is much bigger than the Alfven velocity V_A. The magnetic field penetration mode provides the basis to such devices as the plasma opening switch [9].

Unstable modes

The two other roots in the MHD limit are:

$$\omega_2 = kV_A\left\{\sqrt{1+\beta} - \frac{\boldsymbol{U}\cdot\nabla\boldsymbol{U}}{2L_n\Omega_i^2(1+\beta)}\frac{L_n\Omega_i}{V_A} + O[\frac{V_A}{L_n\Omega_i}]\right\},$$

and

$$\omega_3 = \frac{k\,\boldsymbol{U}\cdot\nabla\boldsymbol{U}}{\Omega_i(1+\beta)}.$$

It is readily seen that mode 3 disappears in inhomogeneous plasma while mode 2 turns into the fast magnetosonic wave.

In the HMHD limit the two roots take the following form:

$$\omega_{2,3} = \frac{1}{2}kL_n\Omega_i\left\{1+\beta+\left(\frac{\boldsymbol{U}\cdot\nabla\boldsymbol{U}}{L_n\Omega_i^2} - \frac{(1+\beta)^2}{4}\right)\left(\frac{L_n\Omega_i}{V_A}\right)^2 \pm i\,2\sqrt{\frac{\boldsymbol{U}\cdot\nabla\boldsymbol{U}}{L_n\Omega_i^2} - \frac{(1+\beta)^2}{4}}\right\}. \tag{3.13}$$

Hence, the growth rate of the instability is given by:

$$\gamma = kL_n\Omega_i\sqrt{\frac{\boldsymbol{U}\cdot\nabla\boldsymbol{U}}{L_n\Omega_i^2} - \frac{(1+\beta)^2}{4}}\;. \tag{3.14}$$

It is apparent from condition (3.14) that in order to obtain an instability the acceleration has to be along the direction of inhomogeneity, as is indeed the case during the compression and expansion stages in z-pinches and capillary discharges. In such situations condition (3.9b) is not satisfied.

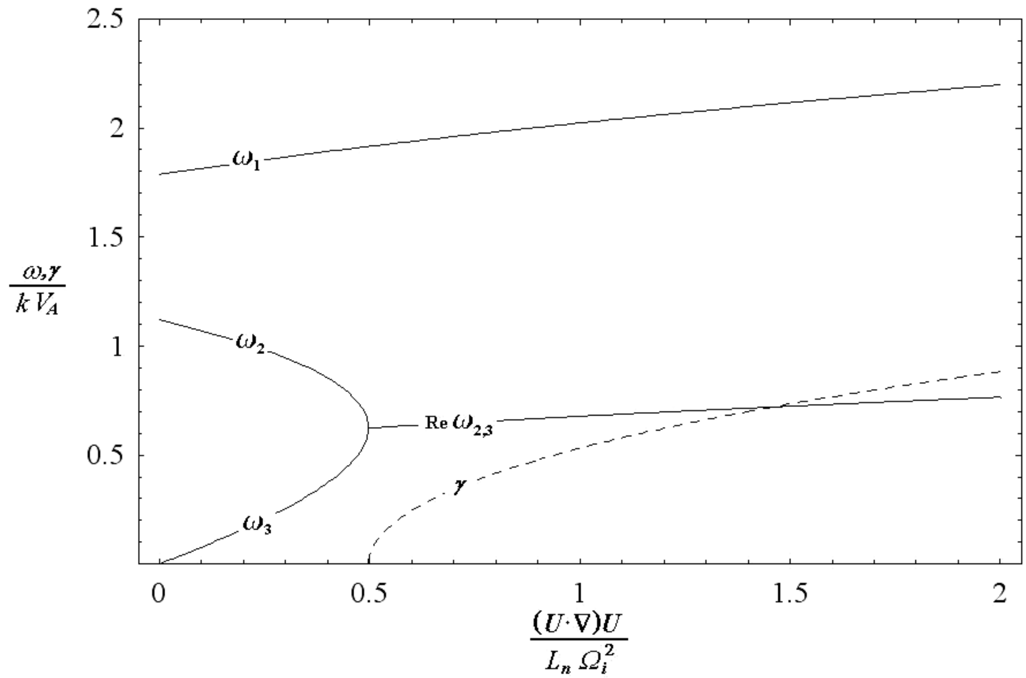

Figure 3.3: The roots of Eq. (3.7) versus dimensionless acceleration $\boldsymbol{U}\cdot\nabla\boldsymbol{U}/L_n\Omega_i^2$.

The parameters for this plot are: $\beta = 1$, $kL_n = 3$, $kV_A/\Omega_i = 2$

It is seen from equation (3.14) and from figure 3.3 that as the inhomogeneity length scale increases, a higher acceleration is needed in order to achieve the instability threshold. This can also be seen from the instability criteria (3.9) and from figure 3.4.

Figure 3.4 represent the dependence of the growth rate on L_n. It is seen from the figure that as hall parameter increases, the growth rate γ increases. This effect of hall parameter on the instability can also be seen from figure 3.2.

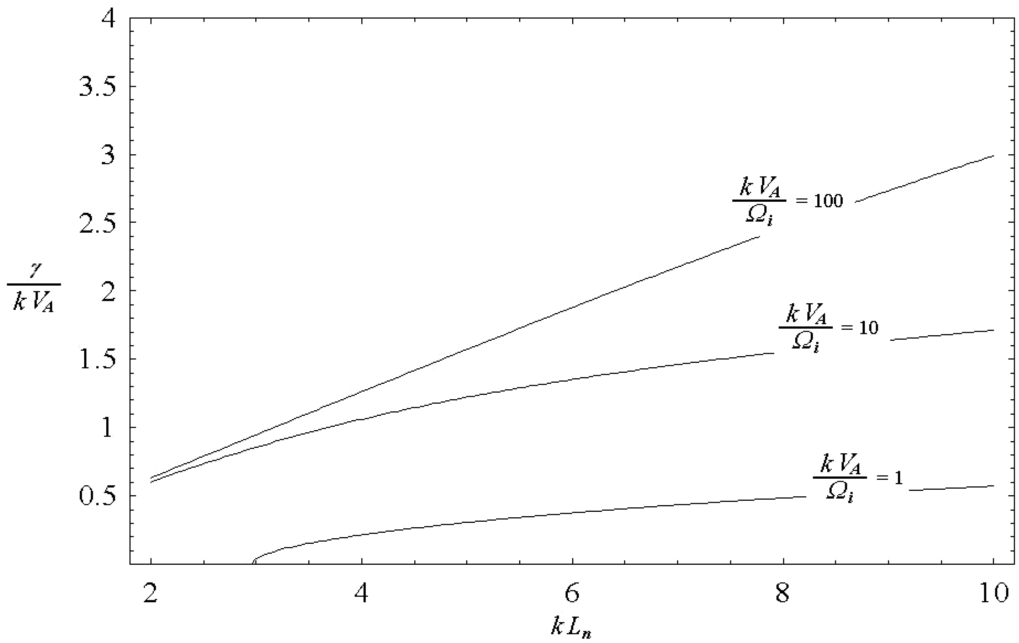

Figure 3.4: The value of the growth rate γ versus the wave number kL_n for different values of hall parameter. The parameters taken for this plot are: $\beta = 0.01$, $U \cdot \nabla U / L_n k^2 V_A^2 = 0.1$

The growth rate γ increases linearly with *k* and tends to infinity in the limit $k \to \infty$. This means that as the wavelength of the perturbation decreases, its growth rate increases without a bound, thus leading to a nonphysical catastrophic behavior. This nonphysical result is resolved when electron mass is re introduced into the HMHD equations. This problem is considered in the next section.

Turning now to determining the properties of modes 2 and 3, we substitute expression (3.13) into (3.6a) – (3.6c) and to lowest order in $L_n\Omega_i/V_A$ obtain:

$$\frac{\rho^1}{\rho} = -\left(\beta - \frac{1}{4}\frac{L_n^2\Omega_i^2}{V_A^2}(1+\beta)^2\right)^{-1}\frac{b_z^1}{B}, \tag{3.15}$$

$$\frac{u_x^1}{u_y^1} \sim -\,4\frac{i}{kL_n}\frac{\beta}{(1+\beta)^2}\frac{V_A^2}{L_n^2\Omega_i^2}. \tag{3.16}$$

From equation (3.15) it is seen that as in the magnetic field penetration mode, the relative perturbations in the ionic fluid are much smaller than those in the electronic fluid. From equation (3.16) it is seen that the ratio of velocity components is a ratio of two large terms, namely $(V_A/\Omega_i L_n)^2$ and kL_n so that the x and y components of the ions velocity are comparable.

The electric field perturbations may be inferred from Faraday's law:

$$\nabla \times \boldsymbol{E}_1 = -\frac{1}{c}\frac{\partial \boldsymbol{B}_1}{\partial t},$$

which results in:

$$-\boldsymbol{k} \times \boldsymbol{E}_1 = \frac{\omega}{c}\boldsymbol{B}_1,$$

and hence

$$E_x^1 = \frac{\omega}{ck} b_z^1 \quad , \qquad E_z^1 = 0 \tag{3.17}$$

Thus, for the two modes, the electric field perturbation lies in the xy plane so that both modes are transverse to magnetic field. The ratio E_x/E_y can be calculated with the aid of the permittivity tensor $[\varepsilon]$ which was defined for the analysis of homogeneous plasmas (2.10):

$$\nabla \cdot \mathbf{D} = \nabla \cdot [\varepsilon]\mathbf{E} = 0. \tag{3.18}$$

The the result is given by

$$\frac{E_x}{E_y} = -i\frac{\varepsilon_1}{\varepsilon_2}, \tag{3.19}$$

where ε_1 and ε_2 are defined in equation (2.11). Substituting the complex root into (3.19) results in:

$$\frac{E_x}{E_y} \propto kL_n\left(\frac{V_A}{c}\right)^2. \tag{3.20}$$

In the limit $V_A^2/c^2 << 1/kL_n$ the y component of the perturbed electric field is much bigger than the x component and hence, the wave is almost linearly polarized in the direction of the wave. This means that $\nabla \times \boldsymbol{E}_1 \sim 0$ so that these waves are almost electrostatic waves.

3.4 Effects of electron inertia

In the previous section it was shown that the growth given in (3.14) increases linearly with k and tends to infinity in the limit $k \to \infty$. In this section we show that this non physical result is resolved when electrons inertia is taken into account. Doing so, equation (2.23b) is modified. Following the same procedure that leads to the result presented in the previous sections, result in replacing ω with $\omega(1 + c^2k^2/\omega_{pe}^2)$ in the three scalar equations that were derived from (2.23b). Hence, equation (3.7) turns into the following modified dispersion equation:

$$\omega^3(1 + k^2c^2/\omega_{pe}^2) + \omega^2 \frac{kV_A{}^2}{\Omega_i L_n} - \omega k^2 V_A{}^2 (1 + \beta(1 + k^2c^2/\omega_{pe}^2)) + \frac{k^3 V_A{}^2}{\Omega_i}(\boldsymbol{U}\cdot\nabla)\boldsymbol{U} = 0. \tag{3.21}$$

This dispersion equation is exactly like the dispersion equation that was considered in the previous section except for the term k^2c^2/ω_{pe}^2 that represents the finite electron's inertia. This quantity is proportional to the electron mass and to the square of the wave number k. It can be neglected if k is small yielding equation (3.17), but should be included for large k's. The complex root of the equation normalized to the ions gyro frequency as a function of kc/ω_{pe} is shown in figure 3.5 for three different values of β. The growth rate (imaginary part) is plotted with a dashed line.

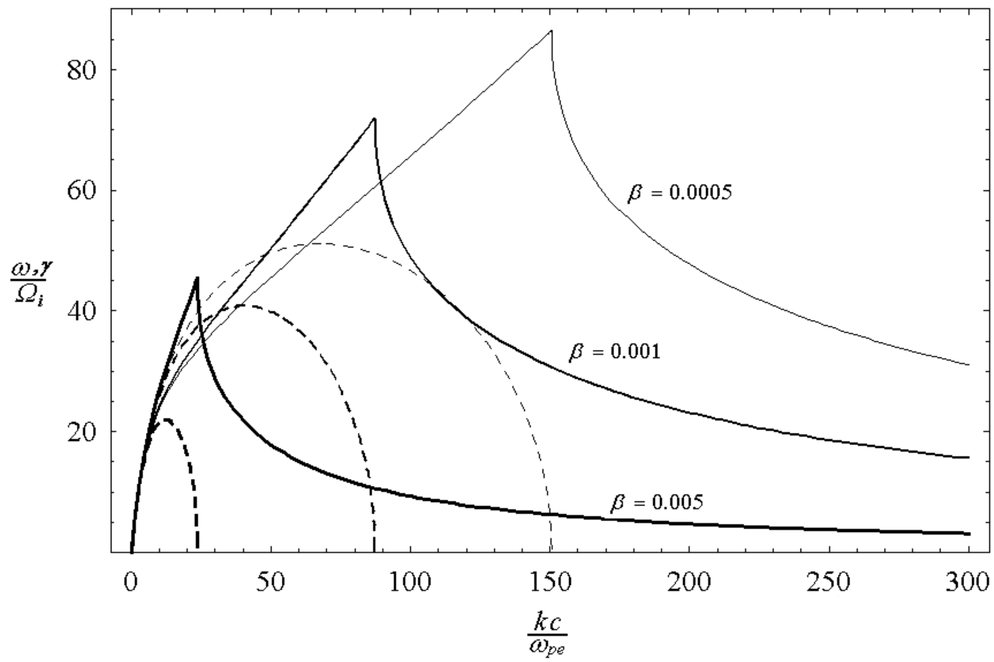

Figure 3.6: The frequency and growth rate normalized with the ions gyro frequency versus the normalized wave number kc/ω_{pe} for different values of β. The parameters for this plot are: $L_n = 4.5$, $V_A = 1.09\times 10^9$, $\omega_{pe} = 5.6\times 10^{10}$, $U\cdot\nabla U = 0.5\,\Omega_i^2 L_n (1+\beta)^2$

It can be seen from figure 3.5 that for a given value of β , the growth rate is zero for wave lengths that are shorter than some nonzero wave length $2\pi / k^*$, that is given by

$$k^* \approx \frac{\omega_{pe}}{c}\sqrt{\frac{2\sqrt{\boldsymbol{U}\cdot\nabla\boldsymbol{U}} - \sqrt{L_n}(1+\beta)\Omega_i}{\sqrt{L_n}\,\beta\Omega_i}} \tag{3.22}$$

Thus, the system is stable for perturbation with $k > k^*$. In addition, a maximum in the growth rate is achieved at a wave length $2\pi / k_{\max}$ which is given by (in the limit $\beta << 1$):

$$k_{\max} \approx \frac{\omega_{pe}}{c}\sqrt{\frac{-2\sqrt{L_n}(1+\beta)\Omega_i + \sqrt{12\boldsymbol{U}\cdot\nabla\boldsymbol{U} + L_n(1+\beta)^2\Omega_i^2}}{3\sqrt{L_n}\,\beta\Omega_i}}\ , \tag{3.23}$$

while the maximal growth rate is:

$$\frac{\gamma_{\max}}{\Omega_i} \approx \frac{\omega_{pe}}{c\Omega_i^2}\sqrt{\frac{\xi_2(\xi_3(\xi_2(5\xi_1-8\xi_2)-\xi_3)+\xi_2^3(\xi_2+\xi_1)}{54\beta(2\xi_2-\xi_1)}} \ , \tag{3.24}$$

where

$$\xi_1=\sqrt{\xi_3+\xi_2^2} \ , \qquad \xi_2=\sqrt{L_n}\mathit{\Omega}_i \ , \qquad \xi_3=12\boldsymbol{U}\cdot\nabla\boldsymbol{U} \ .$$

It is easy to see from equations (3.22)-(3.24) and figure 3.5 that for smaller β the system will be more unstable with bigger maximal growth rate and for a wider range of wave lengths. Thus, the plasma thermal pressure has a stabilizing effect on the hall instability. In the limit of $k^2c^2/\omega_{pe}^2 << 1$ and finite *k*, the quantities k^*, $k_{\max}$ and γ tend to infinity, in accordance to the analysis in the previous sections.

In HMHD limit ($V_A/\Omega_i L_n >> 1$), the condition for instability is modified and takes the following form:

$$\boldsymbol{U}\cdot\nabla\boldsymbol{U} > \frac{1}{4}L_n\mathit{\Omega}_i^2(1+\beta)^2(1+\beta k^2c^2/\omega_{pe}^2)\,, \tag{3.25}$$

which differs from (3.9a) only by the $\beta k^2c^2/\omega_{pe}^2$ term. It is easily seen from (3.25) that in the range of short wave lengths, where the term k^2c^2/ω_{pe}^2 must be taken into account, β make the instability condition harder to achieve and hence, increasing the pressure has a stabilizing effect.

3.5 Wave propagation almost perpendicular to magnetic field

So far waves that propagate perpendicular to the magnetic field have been considered. It was shown that such waves are unstable under certain conditions. In this section it will be shown that these waves are the most unstable among all waves whose direction of propagation is in small vicinity around perpendicular propagation. The geometry remains the same except for the wave vector which now forms a small angle δ with the y axis as shown in figure 3.6.

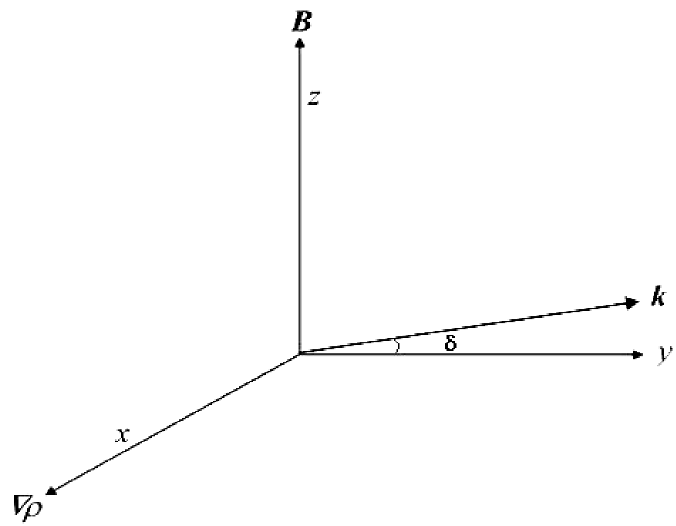

Figure 3.7: The wave vector now forms a small angle δ with the y axis

$$\boldsymbol{k} = k_y \hat{y} + k_z \hat{z} = k(\cos\delta\,\hat{y} + \sin\delta\,\hat{z}) \approx k\hat{y} + k\delta\hat{z}$$

The perturbations are written in the following form:

$$\begin{aligned}
\boldsymbol{B}_1 &= (b_x^{\ 1}\hat{x} + b_y^{\ 1}\hat{y} + b_z^{\ 1}\hat{z})e^{i(ky+\delta kz-\omega t)} \\
\boldsymbol{U}_1 &= (u_x^{\ 1}\hat{x} + u_y^{\ 1}\hat{y} + u_z^{\ 1}\hat{z})e^{i(ky+\delta kz-\omega t)} \qquad (3.26) \\
\rho_1 &= \rho^1 e^{i(ky+\delta kz-\omega t)}
\end{aligned}$$

Inserting (3.26) into equations (2.21a) - (2.21c), linearizing around the unperturbed state and neglecting terms proportional to $1/L_n$ with respect to k, results in a linear and homogeneous set of equations. The condition for the existence of non trivial solution results in the following dispersion equation that provides a relationship between ω and k::

$$\omega^4 - \frac{k(L_n(\boldsymbol{U}\cdot\nabla)\boldsymbol{U} + V_A^2(\beta-1))}{L_n\Omega_i}\omega^3 - \frac{k^4V_A^4}{\Omega_i^2}\left(\frac{L_n(\boldsymbol{U}\cdot\nabla)\boldsymbol{U} + V_A^2\beta + L_n^2\Omega_i^2(1+\beta)}{k^2L_n^2V_A^2} + \delta^2\right)\omega^2 + \frac{k^3V_A^2(V_A^2\beta(1+\beta) + L_n(\boldsymbol{U}\cdot\nabla)\boldsymbol{U}\,(2+\beta))}{L_n\Omega_i}\omega + \frac{k^6V_A^6\beta}{\Omega_i^2}\left(\delta^2 - \frac{(\boldsymbol{U}\cdot\nabla)\boldsymbol{U}\,(L_n(\boldsymbol{U}\cdot\nabla)\boldsymbol{U} + V_A^2\beta)}{k^2L_nV_A^4\beta}\right) = 0 \tag{3.27}$$

In the limit $\delta \to 0$, equation (3.27) is simplified and can be written as follows:

$$\left\{\omega - k\frac{V_A^2}{\Omega_i}\left(\frac{(\boldsymbol{U}\cdot\nabla)\boldsymbol{U}}{V_A^{\,2}} + \frac{\beta}{L_n}\right)\right\}\left\{\omega^3 + \omega^2\frac{kV_A^{\,2}}{\Omega_iL_n} - \omega k^2V_A^{\,2}(1+\beta) + \frac{k^3V_A^{\,2}}{\Omega_i}(\boldsymbol{U}\cdot\nabla)\boldsymbol{U}\right\} = 0 \tag{3.28}$$

Equation (3.28) corresponds to the dispersion equation obtained in the problem of orthogonal propagation which was discussed in previous section.

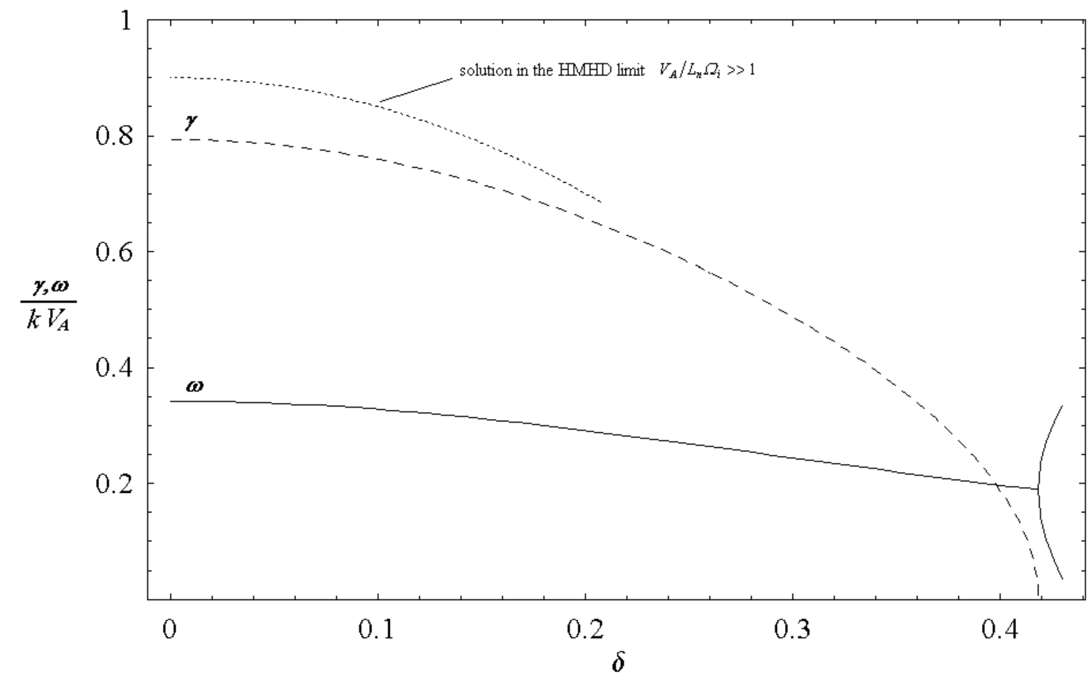

Figure 3.8: The frequency ω and the growth rate γ of the unstable mode as a function of the angle δ. The dotted line represents the solution in the limit $V_A/L_n\Omega_i >> 1$. The parameters for this plot: $\beta = 1$, $k = 0.6$, $L_n = 5$, $kV_A/\Omega_i = 10$, $\Omega_i = 4.8\times10^7$, $(\boldsymbol{U}\cdot\nabla)\boldsymbol{U} = 0.1L_n k^2 V_A^2$

Thus, for a given *k*, it is readily seen that the maximum growth rate is attained for perpendicular propagation, i.e, $\delta = 0$. Furthermore the growth rate decreases as δ is increased until it reaches zero for a finite δ. Beyond that angle, the system is stable. In order to obtain an estimate of the stabilizing effect of δ, the frequency ω is expanded in taylor series in δ around zero:

$$\omega = \omega_0 + \omega_1\delta + \omega_2\delta^2 + ..., \tag{3.29}$$

where ω_0 is the frequency that corresponds to $\delta = 0$ which is known from the previous chapter. Substituting (3.29) into (3.27), and taking ω_0 to be the complex root from previous chapter yields:

$$\omega_1 = 0$$

Taking the HMHD limit $V_A / L_n \Omega_i >> 1$ for ω_2 results in:

$$\omega_2 = \mp i \frac{k^3 L_n^3 \Omega_i}{\sqrt{\frac{4(\boldsymbol{U} \cdot \nabla)\boldsymbol{U}}{L_n \Omega_i^2} - (1+\beta)^2}} \left(\frac{V_A}{L_n \Omega_i} \right)^2 \left\{ 1 + O[\left(\frac{L_n \Omega_i}{V_A} \right)^2] \right\} \tag{3.30}$$

The $\pm$ signs correspond to the $\mp$ signs of the imaginary part of the complex root so it decreases the growth rate which has a maximum for $\delta = 0$. Thus, equation (3.30) demonstrates the stabilizing effect of a small deviation from exact perpendicular propagation. The approximated solution for almost perpendicular propagation in the HMHD limit ($V_A / L_n \Omega_i >> 1$) may be given by $\omega = \omega_0 + \omega_2 \delta^2$ and is shown in dotted line in figure 3.8.

4. Three dimensional oblique wave

4.1 Basic model and assumptions

In this section, a first step is made towards a comprehensive study of wave propagation in inhomogeneous HMHD plasmas such that the wave vector has non vanishing component along any of the three axes. Thus, the same geometry as presented in the previous section is considered, with the different that now the wave vector is characterized by three arbitrary angles it forms with the three axes. The cosines of those angles are denoted by l_x, l_y, l_z, and all three are assumed to be of the same order.

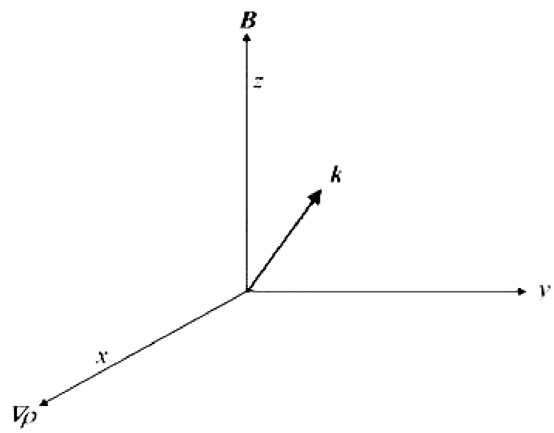

Figure 3.1: The wave vector is characterized by three arbitrary angles it forms with the axes.

$$\boldsymbol{B} = B(x)\hat{k}, \qquad \rho = \rho(x), \qquad \boldsymbol{k} = k_x\hat{x} + k_y\hat{y} + k_z\hat{z} = k(l_x\hat{x} + l_y\hat{y} + l_z\hat{z})\,.$$

The perturbations are written in the following form:

$$\boldsymbol{B}_1 = (b_x{}^1\hat{x} + b_y{}^1\hat{y} + b_z{}^1\hat{z})e^{ik(l_x y + l_y y + l_z z) - i\omega t},$$
$$\boldsymbol{U}_1 = (u_x{}^1\hat{x} + u_y{}^1\hat{y} + u_z{}^1\hat{z})e^{ik(l_x y + l_y y + l_z z) - i\omega t}, \qquad (4.1)$$
$$\rho_1 = \rho^1 e^{ik(l_x y + l_y y + l_z z) - i\omega t}.$$

Inserting (4.1) into equations (2.19a) - (2.19c), linearizing around the basic state results a set of 7 equations:

$$-i(B'kl_y V_A^2 + \omega\Omega_i B)b_x^1 + iBV_A^2 k^2 l_z^2 b_y^1 - BV_A^2 k^2 l_y l_z b_z^1 + iB^2\Omega_i kl_z u_x^1 \qquad (4.2a)$$

$$BV_A^2(B'/L_n + iB'kl_x - Bk^2 l_z^2 - B'')b_x^1 - iB^2\omega\Omega_i b_y^1 + Bkl_z V_A^2(iB' + Bkl_x)b_z^1$$
$$+ iB^3\Omega_i kl_z u_x^1 - 4iB'kl_z\pi V_A^4\rho^1 = 0 \qquad (4.2b)$$

$$B^2k^2 l_y l_z V_A^2 b_x^1 - Bkl_z V_A^2(iB' - iB/L_n + Bkl_x)b_y^1 - iB^2(kl_y V_A^2/L_n + \omega\Omega_i)b_z^1$$
$$+ B^2\Omega_i(B' - iBkl_x)u_x^1 - iB^3\Omega_i kl_y u_y^1 + 4\pi iB'kl_y V_A^4\rho^1 = 0 \qquad (4.2c)$$

$$iBkl_z V_A^2 b_x^1 + V_A^2(B' - iBkl_x)b_z^1 - iB^2\omega u_x^1 = 0 \qquad (4.2d)$$

$$-Bkl_z V_A^2 b_y^1 + Bkl_y V_A^2 b_z^1 + 4\pi\beta V_A^4 kl_y\rho^1 + B^2\omega u_y^1 = 0 \qquad (4.2e)$$

$$B'V_A^2 b_x^1 + i4\pi\beta V_A^4 kl_z\rho^1 + iB^2\omega u_z^1 = 0 \qquad (4.2f)$$

$$B^2(1/L_n - ikl_x)u_x^1 - iB^2 kl_y u_y^1 - iB^2 kl_z u_z^1 - i4\pi V_A^2\omega\rho^1 = 0 \qquad (4.2g)$$

4.2 Solution

The condition for having non trivial solutions for the linear homogeneous set of equations (4.2a) – (4.2g) is that the determinant of the matrix of coefficient is zero. Inspecting equations (4.2a) – (4.2g) reveals that that determinant may be written as:

$$D(\omega,k)=\left|-i\omega\mathrm{U}+k^2 l_z\mathrm{H}+ik\mathrm{A}+\frac{1}{L_n}\mathrm{B}\right| , \tag{4.3}$$

where U, H, A and B are 7×7 matrices that contain functions of the unperturbed state and the direction cosines. In particular, A and B contains terms that result from the inhomogeneity of the plasma. The significant different between the perpendicular propagation ($l_z=0$) and the general case is immediately obvious. Assuming that k is large (in the sense discussed in the previous section), the former case is characterized by a linear relationship between ω and k, while the dominant term in the latter case is the one proportional to H and thus making ω proportional to k^2. Consequently, the frequency ω is expanded in a power series in the following way:

$$\omega=\omega_0 k^2+\omega_1 k+\omega_2+\dots . \tag{4.4}$$

Substituting (4.4) into the dispersion relation (4.3) yields a 14th order polynomial in k. The condition for non trivial solution is that each coefficient of this polynomial is zero. Solving for the highest order in k results:

$$\omega_0=\pm\frac{l_z V_A^2}{\Omega_i} . \tag{4.5}$$

This solution represents the whistler modes that are of electronic nature. This may be seen by substituting (4.5) into (4.2a) - (4.2g). Leaving only terms which proportional to k^2 results in:

$$u_x^1 = u_y^1 = u_z^1 = \rho^1 = 0\,,$$

$$b_x^1 = \frac{il_y - l_x l_z}{1 - l_z^2} b_z^1\,,$$

$$b_y^1 = -\frac{il_x - l_y l_z}{1 - l_z^2} b_z^1\,.$$

For high order of k, the only perturbations are of the magnetic field, other perturbations including density are of smaller order. Taking into account that the magnetic field is frozen into the electron fluid, this wave is an electron wave for first order approximation. It may be seen from equation (4.5), that unlike the perpendicular propagation case, the whistler mode exist in the oblique case also in homogeneous plasmas. As was describes in the previous section, the whistler modes reemerges in a modified form in the case of perpendicular propagation due to the plasma inhomogeneity. They were termed also fast magnetic penetration mode and were found to be unconditionally stable. In order to investigate the effect of the plasma inhomogeneity on the oblique whistler modes, the next order contributions to ω are calculated. The result is given by:

$$\omega_1 = -\frac{l_y (L_n (\boldsymbol{U}\cdot\nabla)\boldsymbol{U} + V_A^2(1-\beta))}{2L_n\Omega_i} - i\frac{l_x l_z (L_n (\boldsymbol{U}\cdot\nabla)\boldsymbol{U} + V_A^2(1+\beta))}{2L_n\Omega_i}$$

Hence, the growth rate is:

$$\gamma = \frac{l_x l_z}{2\Omega_i} k \left[(\boldsymbol{U}\cdot\nabla)\boldsymbol{U} + \frac{V_A^2(1+\beta)}{L_n} \right] \qquad (4.6)$$

The growth rate (4.6) vanishes for homogeneous plasma but if the plasma has no acceleration and still inhomogeneous we will still have instability. In that case this instability will be of the order $kV_A^2 / \Omega_i^2 L_n$. In the MHD limit This quantity will be very small hence, the growth rate will be very small.

5. Summary

HMHD waves and instabilities in accelerating non homogeneous plasmas have been investigated. In contrast to the MHD model, where both ions and electrons are magnetized, the HMHD model is defined for regimes where electrons are magnetized and ions are unmagnetized, i.e, $\Omega_i << \omega << \Omega_e$. The two fluid equations were used, neglecting the contribution of electrons inertia (which defines the upper bound on the frequency regime). The problem of waves orthogonal to magnetic field and density gradient was considered. Linearizing around the basic state we have obtained a set of linear equations for the perturbation. Assuming that the wave length of the wave is much smaller than the inhomogeneity scale length, and looking for non trivial solution a relation between ω and k (dispersion equation) has been obtained. This dispersion equation was obtained also in [2] and is the same dispersion relation obtained in [1] and [4] for zero acceleration.

The dispersion relation has three roots that represent three branches of wave propagation. One of the branches is always stable, is related to the electrons, and has developed from the fast magnetosonic mode as a result of the plasma's inhomogeneity. This mode is a modified Whistler mode and provides the mechanism for fast non dissipative penetration of magnetic field into the plasma. The same root is obtained and discussed in [4]. One of the two other branches also obtained from the fast magnetosonic wave and when the acceleration is big anough, it merges with the third branch, which is a new branch, into a pair of complex conjugate modes one of which is unstable. The unstable mode was found to be an electrostatic wave with growth rate that proportional to ions acceleration. This growth rate is maximized when the wave is orthogonal to the magnetic field.

This unstable mode has a growth rate that is proportional to the wave number k. For $k \to \infty$ the growth rate tends to infinity which leads to catastrophic instability. This problem is then ill-posed which is resolved when taking into account electron inertia. Consequently it was found that the instability exists for a definite range of wave lengths and that the growth rate exhibits a maximum at a certain wave length. This maximum is found to decrease in higher a temperature which also reduces the range of wave length for which the instability exists.

Further discussion is made for oblique three dimensional waves. Expanding the frequency in a power series in the wave number *k* and i.e, short wave lengths, it was shown that the lowest order produced the Whistler mode whose frequency is proportional to k^2 while the next order solution demonstrates that the plasmas inhomogeneity gives rise to an instability of the whistler mode whose growth rate is proportional to *k*.

References

[1] Brushlinskii, K.V. and Morozov, A.I. In: *Reviews of Plasma Physics*, edited by M. A. Leontovich, (Consultant Bureau, New York, 1980), Vol.**8**, 122

[2] Huba, J.D. *Phys. Fluids*., **B2**, 3217, (1991)

[3] Hassam, A.B. and Huba, J.D. *Phys. Fluids*., **31**, 318, (1988)

[4] Almaguer, J.A. *Phys. Fluids*., **B4**, 3443, (1992)

[5] P. Zhu, A. Bhattacharjee, and Z.W. Ma, *Phys. Plasmas*., **10(1)**, 249, (2003)

[6] A. Fruchtman, *Phys. Fluids*., **B3**, 1908, (1991)

[7] R. Arad, K. Tsigutkin, Y. Maron, A fruchtman, and D. Huba , *Phys. Plasmas.,* **10(1)**, 112, (2003)

[8] F.Chen, *Plasma Physics*, Plenum Press, New York, 1974.

[9] N. A. Krall and A. W. Trivelpiece, *Principles of Plasma physics*, Mcgraw-Hill, 1973.

[10] A.I. Akhiezer, *Plasma Electrodynamics*, Pergamon Press, New York, 1975.

תקציר

עבודה זו עוסקת בחקר גלים ואי יציבות הול בזרימות פלסמה בעלות מוליכות אין סופית. המשוואות המשמשות לתיאור הפלסמה הן משוואות HMHD, המאופיינות על ידי תדירות אופיינית שהיא גבוהה מתדירות הציקלוטרון של היונים ואשר איבר הול נכלל בהן בחוק פרדיי. להתקדמות גלים בניצב לשדה המגנטי ולאי ההומוגניות של הפלסמה, קיימים שלושה אופני התקדמות שונים, כאשר אחד מהם יציב תמיד ואילו השניים האחרים עלולים להיות לא יציבים בהשפעת תאוצת היונים. נמצא כי הגל היציב ואחד משני הגלים הלא יציבים מתפתחים מהגל המגנטוסוני המהיר ואילו הגל השלישי נעלם בפלסמה הומוגנית. הגל היציב נראה הינו סוג של גל Whistler ותכונותיו נחקרות בעבודה זו. עבור אי היציבות של שני הגלים האחרים, הנובעת מתאוצת הפלסמה, נמצאו ביטויים לסף אי היציבות ולקצב הגידול שלה כפונקציה של מספר הגל ושל סקלת האורך של אי ההומוגניות של הפלסמה. קצב הגידול פרופורציוני למספר הגל דבר שעלול לגרום לאי יציבות קטסטרופית בגבול של אורכי גל קצרים. בעיה זו ניתנת לפיתרון עם התחשבות במסת האלקטרונים. נמצא שכאשר מסת האלקטרונים נלקחת בחשבון, ניתן למצוא אורך גל סופי בו קצב הגידול מכסימלי ובנוסף שונה מאפס לטווח סופי של אורכי גל. עוד נמצא כי הכיוון הניצב לכיוון השדה המגנטי הוא הכי פחות יציב להתקדמות גלים תחת סטייה של זוויות קטנות מכיוון זה. בנוסף נחקרת התקדמות של גלים בזווית כל שהיא לכיוון השדה המגנטי ונמצא שגל Whistler הופך ללא יציב כתוצאה מאי הומוגניות הפלסמה.

אוניברסיטת בן-גוריון בנגב
הפקולטה למדעי ההנדסה
המחלקה להנדסת מכונות

אי יציבות הול בזרימות פלסמה

חיבור זה מהווה חלק מהדרישות
לקבלת התואר "מגיסטר" בהנדסה

מאת: זהר קולברג

מנחה: פרופ' מיכאל מונד

מחבר:	תאריך:
מנחה:	תאריך:
יו"ר ועדת מוסמכים:	תאריך:

שבט תשס"ד **ינואר 2004**

אוניברסיטת בן-גוריון בנגב
הפקולטה למדעי ההנדסה
המחלקה להנדסת מכונות

אי יציבות הול בזרימות פלסמה

חיבור זה מהווה חלק מהדרישות
לקבלת התואר "מגיסטר" בהנדסה

מאת: זהר קולברג

שבט תשס"ד **ינואר 2004**